# Combined Application of Er:YAG and Nd:YAG Lasers Enhances Osseointegration at Dental Bone-Implant Interface

Tianyuan Zhao and Meihua Li*

Department of Stomatology, The Second Hospital of Jilin University, Changchun, China

The combination of a bone and an implant surface is a dynamic biological process. By improving the osseointegration efficiency of the bone tissue around the implant surface, the implant can obtain long-term stability. In this study, we have investigated the potential applications of dual-wavelength lasers (Er:YAG laser and Nd:YAG laser) in implantations and observed their possible efficacy in promoting tissue repair around the implant. The animal experimental model of a rabbit femoral defect implant was used to simulate the process of tissue reconstruction around the implant in humans. The results indicated that by micro-CT observation, it was obvious that the bone mineral density (BMD) values of the dual-wavelength laser group were significantly higher than those of other groups. Furthermore, VG staining clearly showed that there was no obvious physiological gap detected between the implant and the surrounding bone tissues in the dual-wavelength laser group. HE staining further revealed that no significant influx of inflammatory cells was observed around the implants. Immunohistochemical staining of OCN and VEGF showed that the positive area percentages of the dual-wavelength laser group were significantly higher than other groups at the same time point. Therefore, the application of a dual-wavelength laser in implantations can exhibit a positive effect on promoting the reconstruction of bone tissues.

Keywords: osseointegration, bone-implant interface, dental implant, micro CT, Er:YAG laser, Nd:YAG laser

## 1 INTRODUCTION

In dental implant surgery, optimal bone integration of an implant and the surrounding tissues constitutes the foundation and focus of implant-supported denture restoration (Albrektsson and Wennerberg, 2019). At present, the surface of implants for clinical application has been generally roughened to increase its biocompatibility with the bone tissues. For instance, studies by Alsaadi et al. (2006) have revealed that titanium implants with rough surfaces have a significantly higher survival rate than titanium implants with traditional machined surfaces. Moreover, an Er:YAG laser that has been approved by the FDA has exhibited good biological effects as a dental hard tissue laser. Therefore, an Er: YAG laser might have good developmental prospects for the treatment of implants and bone tissue surfaces (Schwarz et al., 2006).

Many previous studies have shown that the surface of bone tissue irradiated by an Er:YAG laser can potentially accelerate the osteoblasts to produce new bones and enhance the retention rate of fibrin and blood clots (Safioti et al., 2017). Moreover, titanium implants treated with an Er:YAG laser

can effectively improve the surface wettability and thereby substantially improve the adhesion of tissue cells for early bone repair (Nejem Wakim et al., 2018). In addition, the research conducted by Kazemzadeh-Narbat et al. (2010) has indicated that the potential application of antibacterial coatings and organic molecules on the implant surface could significantly reduce the generation of dental plaque biofilm. However, the implant stability could not be achieved on the implant surface by physical adsorption, and moreover, the biological safety still remains to be verified. However, the use of Er:YAG laser irradiation on the implant and the surrounding bone tissues *via* the photothermal effect has been found to be relatively safe and can demonstrate efficient bactericidal effects (Romanos et al., 2019). The Er:YAG laser also displayed significant bactericidal activity against Gram-negative anaerobes (Kreisler et al., 2002). The Er:YAG laser is currently being used clinically for the treatment of peri-implantitis to efficiently remove the dental plaques on the implant surface without affecting the implant surface structure (Ali et al., 2020). For example, Crippa et al. (2020) have reported the use of the Er:YAG laser to treat patients with immediate dental implant infection and obtained a success rate of 94.6%.

The Nd:YAG laser primarily acts on tissues such as dyes and hemoglobin (Mordon et al., 2003) and can be used for rapid coagulation and the treatment of soft tissue inflammation during implant surgery to reduce the time of implant surgery (Evrard et al., 1996). At the same time, the Nd:YAG laser can display the function of rapidly generating photothermal and photochemical effects after being absorbed by the biological tissues and, thus, can rapidly eliminate deeply embedded bacteria (Mellado-Valero et al., 2013). In addition, the Nd:YAG laser low-intensity laser treatment (LLLT) can also significantly promote the proliferation and maturation of human osteoblasts (Li et al., 2017) and accelerate the formation and metabolism of new bones at an early period (Karoussis et al., 2017). However, during clinical applications, the irradiation time and dose of the Nd:YAG laser should be strictly controlled to avoid extensive damage being caused to the surrounding soft and hard tissues (Van Nimwegen et al., 2008). Therefore, in this study, we have used a combination of the Er:YAG laser and the Nd:YAG laser in animal implant surgery to analyze the potential improvement of the early inflammatory response of the tissues around the implant and the possible effects on bone tissue repair after the combination of two-wavelength lasers, which will provide a theoretical basis for the application of the Er:YAG laser and Nd:YAG laser together in oral implant surgery.

## 2 EXPERIMENTAL SECTION

### 2.1 Materials and Apparatus
The Fotona LightWalker AT dual-wavelength laser system, H14-N hand tool, and R21-C2 hand tool were supplied by FT medical (Beijing, China). The Surgic XT Plus, Straumann planting implement, and Straumann sandblasted with large grits and acid-etched (SLA) bone level implant (φ3.3 mm NC, SLA 8 mm) were obtained from Straumann (Beijing, China). Coolabar (Beijing, China) supplied paraformaldehyde and

phosphate-buffered saline (PBS). OCN and VEGF used for immunohistochemistry were purchased from Abcam (Cambridge, United Kingdom). Van Gieson's (VG) solution and the hematoxylin-eosin/HE staining kit were purchased from Solarbio (Beijing, China). Saline was supplied by DZ medicine (Tianjin, China).

### 2.2 Preparation of Two-Wavelength Laser Application Parameters
In this experiment, a Fotona dual-wavelength laser treatment system was used to assist the implantation surgery as shown in **Schemes 1**. First, the instrument was turned on, and the Hc14-N hand tool, R21-C2 hand tool, and tapered fiber tip were connected, respectively. The first therapeutic parameters of the Er:YAG laser (2,940 nm) were set as SSP, 120 mJ, and 15 Hz for cortical bone drilling. The treatment of cortical bone with the Er:YAG laser results in a significant reduction in the risk of cortical bone fracture and improved the initial stability of the implant (Matys et al., 2018). The second therapeutic parameter of the Er:YAG laser (2,940 nm) was set as SP, 80 mJ, and 15 Hz for laser washing at the bone interface. The washing effect of the Er:YAG laser on the implant socket can effectively improve the osseointegration efficiency around the implant (Kesler et al., 2006). The first treatment parameter of the Nd:YAG laser (1064 nm) was set as VLP, 20 Hz, and 4 W for coagulation in implant surgery. The second therapeutic parameter of the Nd:YAG laser (1,064 nm) was set as MSP, 15 Hz, and 1.5 W to improve postoperative bone integration. The Nd:YAG laser can effectively promote the efficiency of new bone formation.(Kim et al., 2015).

### 2.3 Preparation of SLA Dental Implants
An SLA titanium implant (φ3.3 mm NC, SLA 8 mm) was selected as the animal experimental implant to verify the effect of the dual-wavelength laser on osseointegration around the implant. The surface treatment of SLA titanium implants is mainly completed by mechanical roughening, sandblasting, and chemical etching. The SLA pure titanium implants after surface roughening have good compatibility with the bone tissue in the early stage (Kim et al., 2008). The titanium implants of Straumann SLA selected in this experiment were tested according to the standard of SEM images before application.

### 2.4 Experiments on Improving Osseointegration by Laser
#### 2.4.1 Establishment of Bone Defect Animal Models
All animal experimental programs were approved by the Animal Care and Use Ethics Committee of Jilin University. In this study, 36 adult Japanese white rabbits (average weight 2 kg, Beijing HFK Biotechnology Co., Ltd., Beijing, China) with large ears were maintained in the feeding room of the Animal Experimental Center of the School of Basic Medical Science, Jilin University (all the animals were fed under the same conditions of light and temperature). In the operation, Straumann planting implements and Surgic XT Plus were used to prepare the implantation fossa in

the lower part of the femoral head of rabbits step by step to simulate the preparation process of bone tissue during dental implantation.

## 2.4.2 Dual-Wavelength Laser-Assisted Implantation of Dental Implants

Thirty-six adult rabbits (average weight 2 kg) were randomly divided into four groups: Er:YAG, Nd:YAG, combination, and control. After skin preparation and towel laying disinfection under anesthesia, a 3-cm linear longitudinal skin incision was made on the lateral side of the femur, and the muscle tissue and periosteum were carefully separated. In the Er:YAG laser group, the implantation sites of the bone tissues were fixed using the Er:YAG laser (SSP, 120 mJ, and 15 Hz) in a non-contact manner. The holes (3.3 mm diameter and 8.0 mm depth) were prepared gradually in a step-by-step manner to 8 mm by using the Straumann planting implement, with 0.9% sodium chloride isotonic solution. Thereafter, the liquid for cooling irrigation was applied to prevent the bone tissue temperature from overheating. Thereafter, during each reaming drill switching, the Er:YAG laser (QSP, 80 mJ, and 15 Hz) was used for laser swing washing of the implant socket two consecutive times. In the Nd:YAG laser group, the holes (3.3 mm diameter and 8.0 mm depth) were prepared gradually step by step to 8 mm, cooled, and then rinsed with 0.9% sodium chloride isotonic solution. The intraoperative assistant used the Nd:YAG laser (VLP, 20 Hz, and 4 W) for further coagulation to ensure a clear operation field. After the operation was conducted, the sutured implant region was irradiated with the Nd:YAG laser (MSP, 15 Hz, and 1.5 W) low-intensity laser therapy (LLLT) for 120 s for three consecutive days, which could significantly reduce wound pain and accelerate wound healing. In the combination laser group, the Er:YAG laser and the Nd:YAG laser were simultaneously used in the laser application manner described previously. In the control group, the holes (3.3 mm diameter and 8.0 mm depth) were prepared gradually step by step to 8 mm, cooled, and then rinsed with 0.9% sodium chloride isotonic solution.

Thereafter, one Straumann implant ($\varphi$3.3 mm NC and SLA 8 mm) was implanted into the same position at the lower end of the femoral head of the rabbits, and the tissues were properly aligned and layer-sutured using a 3–0 nylon suture at the operation site. All the procedures were performed by the same physician without selective bias. After the surgery on animals, gentamicin was administered at (0.1 ml/kg) with antibiotic medication for 3 days.

### 2.4.3 Micro-CT Analysis

The specimens were scanned by micro-CT (90 kV, 114 mA, and 18 μm image pixel size) to evaluate the effect of bone regeneration and osseointegration. A cylinder (4.0 mm diameter and 8 mm height) was selected as the region of interest (ROI). The 3D reconstruction was performed by multimodal 3D visualization software (NRecon 1.7.1.0 software, Kontich, Belgium). The quantitative analysis of the ROI was conducted by micro-CT auxiliary software (VGStudio Volume Graphics GmbH, Germany), including bone mineral density (BMD, g/cm3), trabecular thickness (Tb. Th, mm), trabecular separation (Tb. Sp, mm), and trabecular number (Tb. N, 1/mm).

### 2.4.4 Histological Evaluation

The samples were immobilized in 4% paraformaldehyde solution for 2 weeks before decalcification for 1 month. The samples were then dehydrated in a series of fractionated ethanol solutions. After vitrification with xylene, the samples were embedded in paraffin wax and cut into slices with 30 μm thickness for VG staining. The inward bone growth was observed *via* an inverted microscope (DSX 500; Olympus Corporation, Tokyo, Japan), and ImageJ was used to analyze the surface area of the newly formed bone tissue. In addition, proximal femurs were immersed in 10% ethylenediaminetetraacetic acid to demineralize for 1 month, after which the specimens were embedded in paraffin and sectioned into 5 μm slices by the microtome. Then, the prepared sections were stained with H&E to investigate the effects of the dual-wavelength laser on bone integration around the implant.

### 2.4.5 Immunohistochemistry

The specimens were fixed in 4% paraformaldehyde for 2 weeks before decalcification for 1 month. After the removal of the implants, the remaining bone tissues were sectioned for an immunohistochemical analysis. In short, the sections were made after a 3% $H_2O_2$ treatment. Then, they were sealed with serum, incubated with primary antibodies and then secondary antibodies, stained, counterstained, and dehydrated. Finally, an optical microscope was used for observation at a magnification of ×100.

## 2.5 Statistical Analysis

Data are presented as mean ± standard deviation. Each group of data was obtained from three independent experiments. Differences between multiple experimental groups were statistically analyzed *via* one-way analysis of variance (ANOVA) and Tukey's multiple comparison test. GraphPad Prism v. 8.2 was used for all statistical analyses. $p < 0.05$ indicated significant difference.

# 3 RESULTS AND DISCUSSION

## 3.1 Microstructural Analysis of Bone Ingrowth

The early process of osseointegration around the implant is related to the activity of endogenous BMSCs. Therefore, dual-wavelength laser-assisted implant surgery is an effective treatment to improve the efficiency of osseointegration around the implant (Yin et al., 2017). Statistical analyses of micro-CT are depicted in **Figures 1A–E**. The Tb. N values of the Er:YAG, Nd:YAG, combination, and control groups in 14 days were 2.26 ± 0.05, 1.96 ± 0.04, 2.56 ± 0.05, and 1.28 ± 0.03 /mm, respectively. It is consistent with the three-dimensional reconstructed image. The bone mineral density (BMD), trabecular separation (Tb. Sp), trabecular number (Tb. N), and trabecular thickness (Tb. Th) of the bone tissues around the implant were calculated for each experimental group. As shown in **Figure 1B**, the BMD of the laser group was significantly greater than that of the control group when compared at the same time ($p < 0.001$), and the bone mineral density of the combined laser group was the largest. However, as shown in **Figure 1C**, the trabecular separation was the smallest in the laser combined treatment group, thereby indicating that the laser combined treatment exhibited the most significant osteogenic effect on bone tissue ($p < 0.001$). The trabecular separation of the Er:YAG laser group was less than that of the constituent bones of the control group, and the trabecular
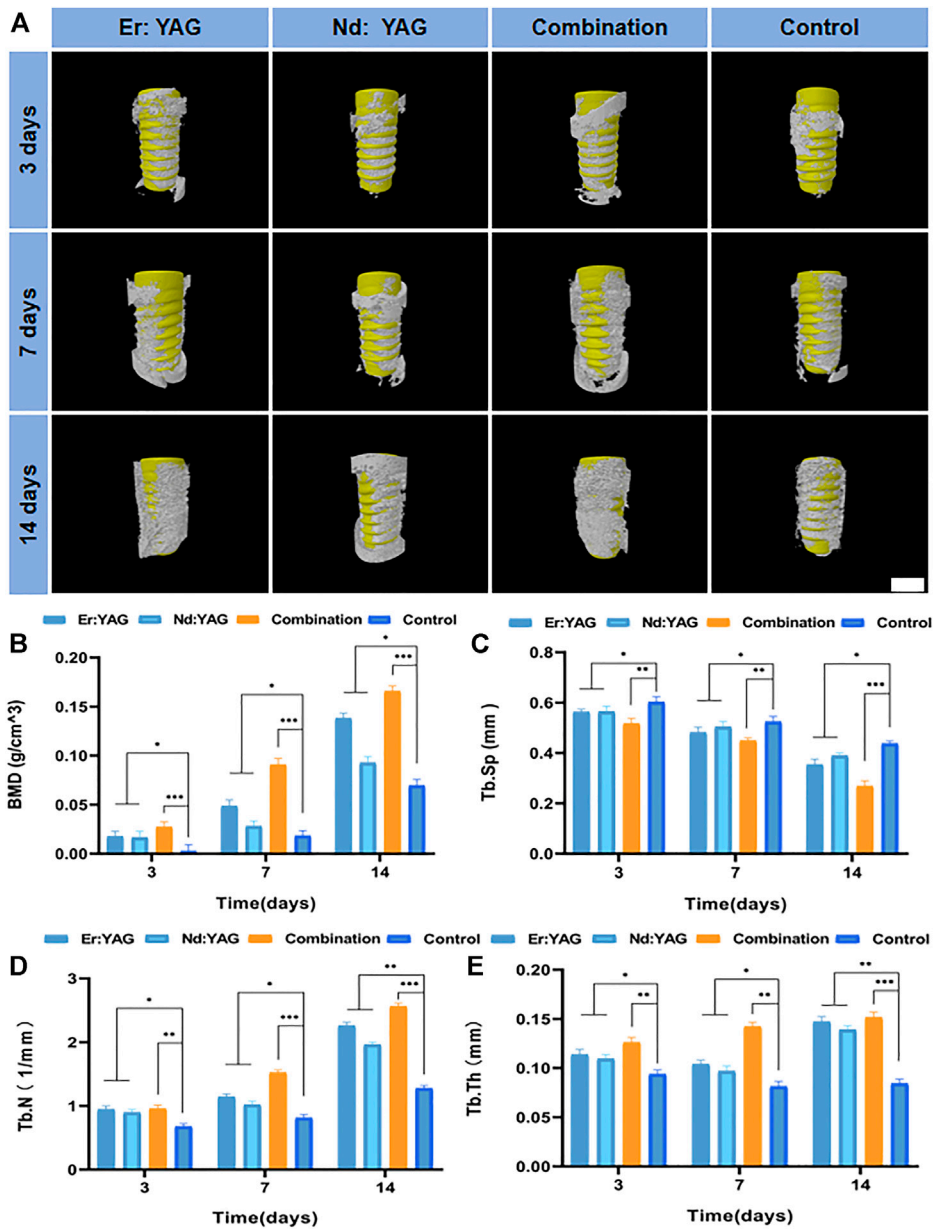
**FIGURE 1 |** Micro-CT analysis of bone integration. **(A)** Representative 3D reconstructed micro-CT images around the implant (scale bar = 4 mm) and the **(B)** BMD, **(C)** Tb. Sp, **(D)** Tb. N, and **(E)** Tb. Th of each group after 3, 7, and 14 days of implantation ($n = 3$, *indicates significant differences between the groups, *$p < 0.05$; **$p < 0.01$; ***$p < 0.001$).

separation in the Nd:YAG laser group was markedly less than that in the control group at 14 days ($p < 0.05$). Overall, based on the data analysis of micro-CT, it could be seen that the combined application of laser resulted in an effective peri-implant bone formation, and the effect was statistically significant ($p < 0.001$).

## 3.2 Osseointegration at SLA Implant Interfaces With Surrounding Bone

The histological results based on HE staining were applied to evaluate the bone integration effect of the peri-implant bone tissue (**Figures**

**2A–C**). As shown in **Figure 2A**, on comparison between the laser group and the control group in 3 days, it could be clearly observed that thermal injury of the bone tissues around implants in the laser group was not significant. The number of inflammatory cells in the bone tissues of the experimental group after Er laser washing treatment was significantly lesser than that of the control group. It was observed that the inflammatory infiltration in the peripheral bone tissues of the Nd laser group was slightly better than that of the control group. However, in the combined laser group, bone integration of the bone tissues around the implant was significant, and there was no necrotic bone tissue area observed on day 3 (**Figure 2A**). Moreover, the laser groups
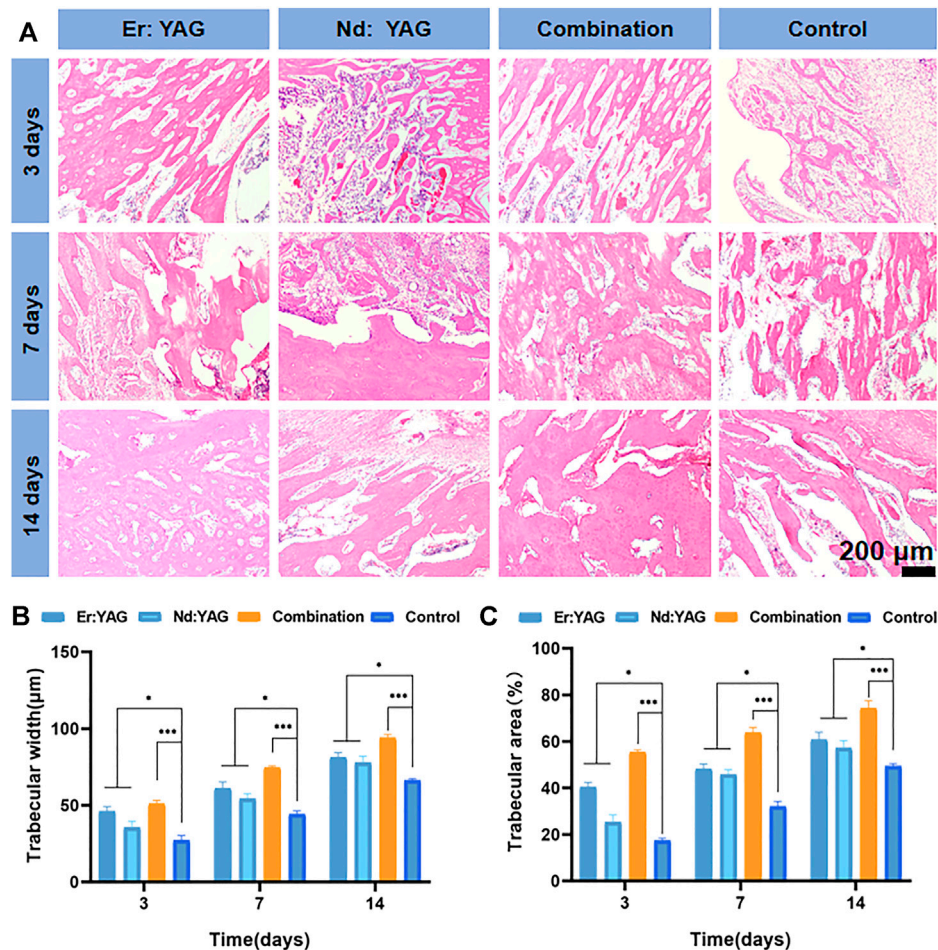
**FIGURE 2 |** Histological analysis of bone integration. Representative images of **(A)** HE staining of the defect site after 3, 7, and 14 days of implantation (pink in HE staining shows collagen fibers of the new bone at the interface between the implant and bone), trabecular width of the regenerated bone **(B)**, and the area of the regenerated bone, following **(C)** HE staining ($n$ = 3, *indicates significant differences between the groups, *$p < 0.05$; **$p < 0.01$; ***$p < 0.001$).

clearly showed that the osteoblasts were surrounded by the bone matrix, and inflammatory infiltration was markedly less than that in the control group in 7 days. These findings suggested that the laser played a positive role during early bone tissue integration (**Figure 2A**). The trabeculae in the laser combined group were clearly visible in 14 days, and they were found to be significantly thicker and denser than those in the other experimental groups and the control group. The thickness and density of the trabecular meshwork in the Er laser group were observed to be superior to those in the Nd laser group (**Figure 2A**). As shown in **Figures 2A and B**, the histological analysis further showed that the osteogenic effect of the laser combined group was substantially superior to that of the control group at all time-points ($p < 0.001$), and it also depicted a novel trend of higher bone formation. In addition, the bone-forming effect of the Er laser was relatively better than that of the Nd laser group.
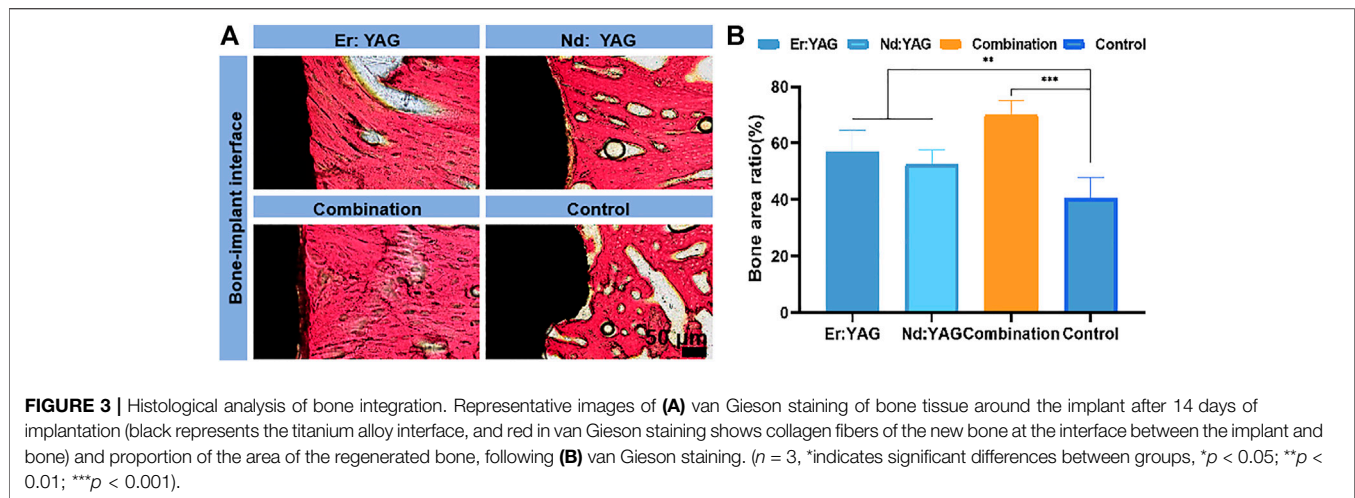
At 14 days, histological data based on van Gieson staining were used to evaluate implant-bone combinations in different experimental groups (**Figures 3A,B**). As shown in **Figure 3A**, on comparing the hard tissue sections of the implants obtained at 14 days, it could be clearly noted that there was no obvious physiological gap between the implant and the surrounding bones in the combination laser group, and the bone repair rate was the highest (**Figure 3B**). In addition, the bone-forming effect of the Er laser was relatively better than that of the Nd laser group. Overall, it could be seen that the combined application of lasers resulted in an effective peri-implant bone formation, and the effect was statistically significant ($p < 0.001$).

## 3.3 Effect of Laser on Osteogenic Differentiation

As shown in **Figure 4A**, the quantitative analysis of immunohistochemical sections of osteocalcin (OCN) clearly showed that the percentage of osteocalcin-positive areas in each group increased significantly with an increase in the number of days. Moreover, the percentage of osteocalcin-positive areas in the laser combined group was significantly higher than that in the other experimental groups and the control group at the same time point, as shown in **Figure 4C**.

Osteocalcin (OCN), also known as bone R-hydroxyglutamic acid protein, is synthesized primarily by osteoblasts and can

**FIGURE 3 |** Histological analysis of bone integration. Representative images of **(A)** van Gieson staining of bone tissue around the implant after 14 days of implantation (black represents the titanium alloy interface, and red in van Gieson staining shows collagen fibers of the new bone at the interface between the implant and bone) and proportion of the area of the regenerated bone, following **(B)** van Gieson staining. ($n = 3$, *indicates significant differences between groups, *$p < 0.05$; **$p < 0.01$; ***$p < 0.001$).

substantially promote early peri-implant bone integration (Mastrangelo et al., 2020). The immunohistochemical results in this study also revealed that the positive expressions of OCN in the Er:YAG, Nd:YAG, and the combination laser groups at 14 days were significantly increased and strikingly higher than those found in the control group (**Figure 4A**). Therefore, an increased positive expression of this important osteogenic marker protein in the peri-implant tissues provided strong evidence for the promotion of new bone formation upon the application of dual-wavelength laser light during implant surgery. This finding also indicated that the combined application of the Er:YAG laser and Nd:YAG laser could markedly promote early bone integration and tissue repair around the implants.

Bone integration and tissue repair in dental implant surgery remain the key factors that can facilitate a successful surgery. For instance, Pourzarandian et al. (2004) have reported that after treatment with the Er:YAG laser, the surface of the bone tissue could effectively promote the adhesion of osteoblasts but did not affect the migration and proliferation of bone tissue cells. The surface of the bone tissue treated with Er:YAG laser swing washing has been found to be associated with several irregularities (Pantawane et al., 2019) such that the bone surface could be more easily adhered to fibrin (Cekici et al., 2013) and thereby effectively promote blood clot stabilization and tissue formation (Niimi et al., 2020). In this experimental study, the bone mineral density (BMD) of the new bone around the implant was analyzed by micro-CT and measurement software. It was clearly observed that the applications of the Er:YAG and Nd:YAG laser groups and these two laser groups in combination were significantly better than those of the control group. Moreover, in the hard tissue sections stained with VG, it could be clearly seen that the space between the implant and the new bone in the Er:YAG, Nd:YAG, and the combination laser groups for 14 days was found to be significantly smaller than that in the control group. Bone binding is a dynamic physiological process (Chang and Giannobile, 2012) and minute movements during the early stages of implantation can negatively affect bone remodeling and generate cicatrix tissue (Sennerby and Meredith, 2008). It has been established

that the larger the contact area between the implant and bone during the early stages, the more significant the impact of bone integration will be. In addition, a number of studies have found that the treatment of cortical bone with the Er:YAG laser and subsequent implantation of the implant can also effectively reduce the risk of bone fractures and adjacent tooth injury around the implant (Matys et al., 2018). It has been observed that the bone tissue treated with the Er:YAG laser can provide better initial stability for the immediate weight-bearing ability of the implant. We also noted that the experimental group using the Er:YAG laser to fix the implantation sites of the bone tissues was significantly superior to the control group based on the effect of bone integration through observations of the tissues under the microscope. A number of previous studies have shown that the Nd:YAG laser postoperative adjuvant treatment of bone defects has a significant role in promoting bone regeneration (Ninomiya et al., 2003). It has also been found that the promotion of bone repair by the Nd laser was primarily due to the biological stimulation of LLLT (Vescovi et al., 2013). For example, Kim et al. (2010) found that the wavelength of the Nd:YAG laser (1064 nm) allowed the laser to effectively penetrate the skin and the different muscle layers and promoted the expressions of BMP-2 and IGF-1 cytokines around bone tissue. Moreover, postoperative irradiation of the wound with the Nd:YAG laser was found to play an important role in mediating bone regeneration (Bouvet-Gerbettaz et al., 2009). Furthermore, HE staining sections of the bone tissues around the implants in this study also indicated that the number and quantity of bone trabeculae around the implants in the laser group were superior to those observed in the control group.

In addition, in this study, the Er:YAG laser was primarily used to fix the implant position, and the 0.9% sodium chloride isotonic solution was used to cool and wash the implants during the dimple washing process, which could significantly avoid thermal damage caused by the laser. A number of studies have shown that excessive bone temperature during implantations can adversely affect the rate of bone tissue incorporation (Trisi et al., 2015). However, the Nd:YAG laser was used in this study to irradiate and induce new bone
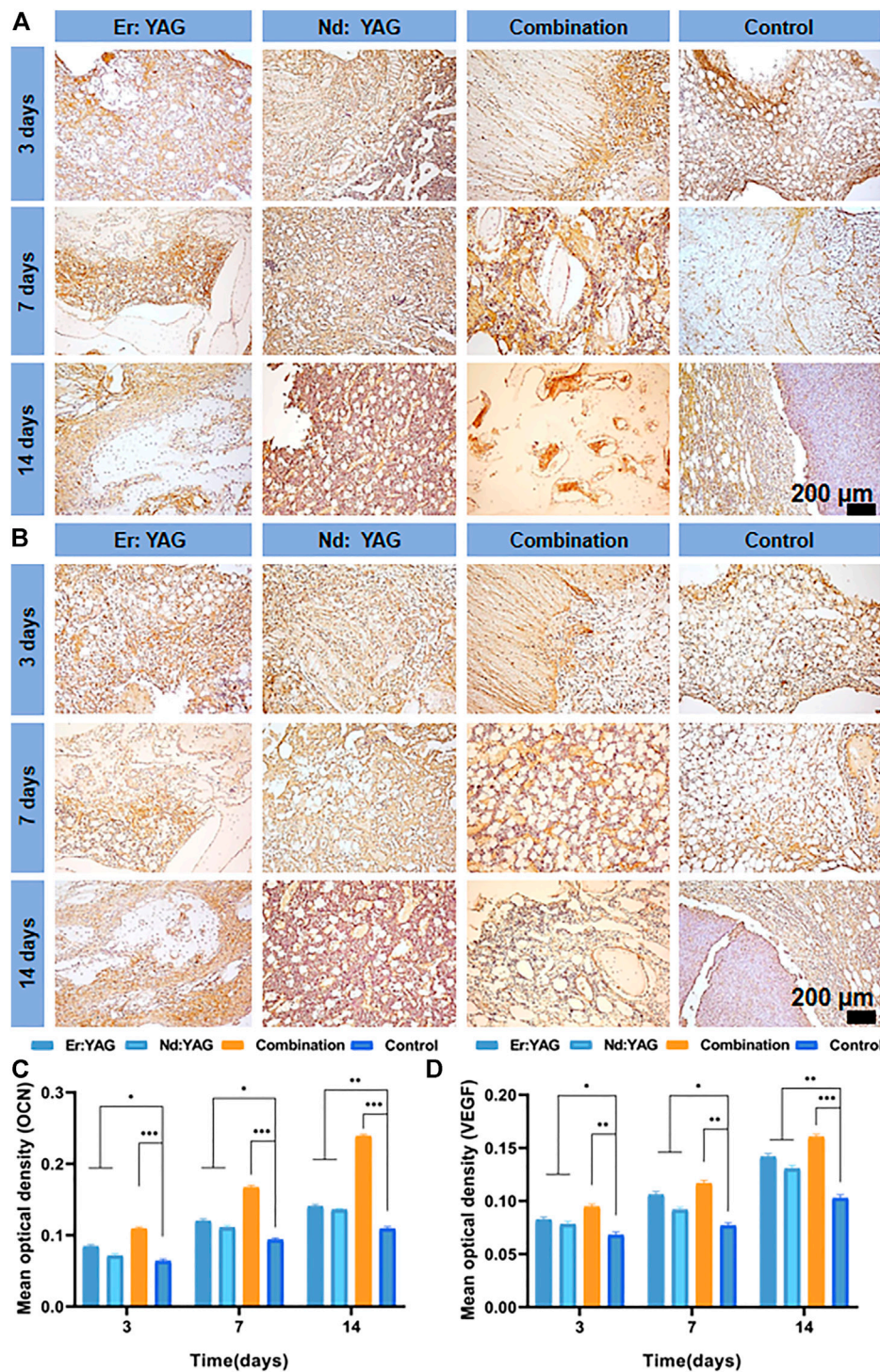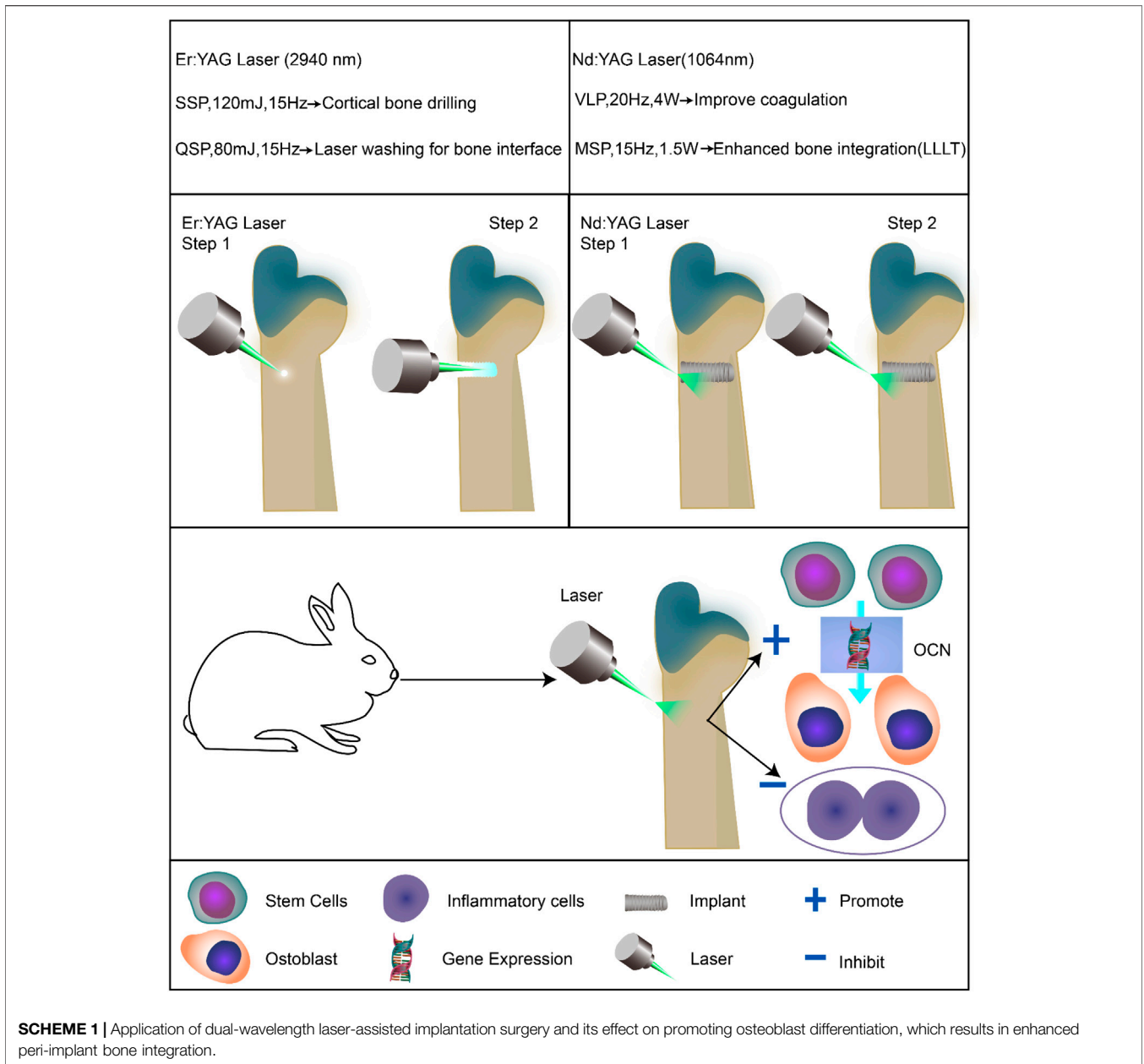
**FIGURE 4 |** Immunohistochemical analysis of the bone around the implant. Representative images of the expressions of **(A)** OCN, **(B)** VEGF, and **(C)** mean optical density of positive areas in the bone around the implants at 3, 7, and 14 days after implantation. ($n = 3$, *indicates significant differences between the groups, *$p < 0.05$; **$p < 0.01$; ***$p < 0.001$).

formation in the implantation area using LLLT low-intensity laser irradiation at an intensity of 1.5 W. Moreover, a previous study by Kim et al. (2015) found that the heat generated by the Nd:YAG laser

at the low power (1.25–2 W) was rather limited, and it could not damage the healthy tissues but exhibited the most significant effects in promoting the repair of the soft and hard tissues around the implants.

**SCHEME 1 |** Application of dual-wavelength laser-assisted implantation surgery and its effect on promoting osteoblast differentiation, which results in enhanced peri-implant bone integration.

## 3.4 Effect of Laser on Vascular Regeneration Around the Bone-Implant Interface

The rate of bone tissue repair around the implants might also be limited by the rate of neo-vascularization in the body (Santos and Reis, 2010). For instance, the vascular endothelial growth factor (VEGF) *in vivo* has a significant angiogenic effect, which can promote the accelerated recovery of the soft and hard tissues around the implant (Zavan et al., 2017).

As shown in **Figure 4B**, the percentage of VEGF-positive areas in each group gradually increased and was found to reach the peak at 14 days. It was observed that the percentage of positive areas in the Er laser group at the same time point was slightly

larger than that in the Nd laser group. The percentage of VEGF-positive areas in the laser combined group was significantly better than in the other experimental groups and the control group, as shown in **Figure 4D** ($p < 0.001$).

## 4 CONCLUSION

In summary, the results of the present study clearly demonstrated the positive effects of early osseointegration of the dental implants upon the application of Er:YAG and Nd:YAG lasers. It was observed that a simultaneous combined application of the Er:YAG and Nd:YAG lasers can achieve the best results for both bone repair and tissue

reconstruction of the implants. These findings of the study thus provide a new clinical method for effectively promoting early bone integration of the implants. However, further clinical trials are needed to also evaluate the potential effects of dual-wavelength laser-assisted implant placement for bone repair.

## DATA AVAILABILITY STATEMENT

The original contributions presented in the study are included in the article/**Supplementary Material**, further inquiries can be directed to the corresponding author.

## ETHICS STATEMENT

The animal study was reviewed and approved by the Animal Care and Use Ethics Committee of Jilin University.

## AUTHOR CONTRIBUTIONS

TZ and ML designed and carried out the experiments and analyzed experimental results. TZ wrote the manuscript. TZ and ML critically reviewed this manuscript and approved the final draft.

## FUNDING

## SUPPLEMENTARY MATERIAL

The Supplementary Material for this article can be found online at: https://www.frontiersin.org/articles/10.3389/fmats.2022.828838/full#supplementary-material

## REFERENCES

Albrektsson, T., and Wennerberg, A. (2019). On Osseointegration in Relation to Implant Surfaces. *Clin. Implant Dent. Relat. Res.* 21, 4–7. doi:10.1111/cid.12742

Ali, S., Salameh, A., Alammory, M., and Hamadah, O. (2020). Comparative Effect of Laser Treatment on Streptococcus Mutans Biofilm Adhered to Dental Implant Surface. *Rese. Jour. Pharm. Technol.* 13 (7), 3311–3316. doi:10.5958/0974-360x.2020.00587.9

Alsaadi, G., Quirynen, M., and van Steenberghe, D. (2006). The Importance of Implant Surface Characteristics in the Replacement of Failed Implants. *Int. J. Oral Maxillofac. Implants* 21 (2), 270–274.

Bouvet-Gerbettaz, S., Merigo, E., Rocca, J. P., Carle, G. F., and Rochet, N. (2009). Effects of Low-Level Laser Therapy on Proliferation and Differentiation of Murine Bone Marrow Cells into Osteoblasts and Osteoclasts. *Lasers Surg. Med.* 41 (4), 291–297. doi:10.1002/lsm.20759

Cekici, A., Maden, I., Yildiz, S., San, T., and Isik, G. (2013). Evaluation of Blood Cell Attachment on Er:Yag Laser Applied Root Surface Using Scanning Electron Microscopy. *Int. J. Med. Sci.* 10 (5), 560–566. doi:10.7150/ijms.5233

Chang, P. C., and Giannobile, W. V. (2012). Functional Assessment of Dental Implant Osseointegration. *Int. J. Periodontics Restor. Dent.* 32 (5), e147–53.

Crippa, R., Aiuto, R., Guardincerri, M., Peñarrocha Diago, M., and Angiero, F. (2020). Effect of Laser Radiation on Infected Sites for the Immediate Placement of Dental Implants. *Photobiomodulation, Photomed. laser Surg.* 38 (3), 186–192. doi:10.1089/photob.2019.4636

Evrard, V. A. C., Deprest, J. A., Van Ballaer, P., Lerut, T. E., Vandenberghe, K., and Brosens, I. A. (1996). Underwater Nd:YAG Laser Coagulation of Blood Vessels in a Rat Model. *Fetal Diagn Ther.* 11 (6), 422–426. doi:10.1159/000264359

Karoussis, I. K., Kyriakidou, K., Psarros, C., Lang, N. P., and Vrotsos, I. A. (2017). Nd:YAG Laser Radiation (1.064 Nm) Accelerates Differentiation of Osteoblasts to Osteocytes on Smooth and Rough Titanium Surfacesin Vitro. *Clin. Oral Impl. Res.* 28 (7), 785–790. doi:10.1111/clr.12882

Kazemzadeh-Narbat, M., Kindrachuk, J., Duan, K., Jenssen, H., Hancock, R. E. W., and Wang, R. (2010). Antimicrobial Peptides on Calcium Phosphate-Coated Titanium for the Prevention of Implant-Associated Infections. *Biomaterials* 31 (36), 9519–9526. doi:10.1016/j.biomaterials.2010.08.035

Kesler, G., Romanos, G., and Koren, R. (2006). Use of Er:YAG Laser to Improve Osseointegration of Titanium Alloy Implants-Aa Comparison of Bone Healing. *Int. J. Oral Maxillofac. Implants* 21 (3), 375–379. doi:10.1016/J.PROSDENT.2006.09.005

Kim, H., Choi, S.-H., Ryu, J.-J., Koh, S.-Y., Park, J.-H., and Lee, I.-S. (2008). The Biocompatibility of SLA-Treated Titanium Implants. *Biomed. Mat.* 3 (2), 025011. doi:10.1088/1748-6041/3/2/025011

Kim, I. S., Cho, T. H., Kim, K., Weber, F. E., and Hwang, S. J. (2010). High Power-Pulsed Nd:YAG Laser as a New Stimulus to Induce BMP-2 Expression in MC3T3-E1 Osteoblasts. *Lasers Surg. Med.* 42 (6), 510–518. doi:10.1002/lsm.20870

Kim, K., Kim, I. S., Cho, T. H., Seo, Y.-K., and Hwang, S. J. (2015). High-intensity Nd:YAG Laser Accelerates Bone Regeneration in Calvarial Defect Models. *J. Tissue Eng. Regen. Med.* 9 (8), 943–951. doi:10.1002/term.1845

Kreisler, M., Kohnen, W., Marinello, C., Götz, H., Duschner, H., Jansen, B., et al. (2002). Bactericidal Effect of the Er:YAG Laser on Dental Implant Surfaces: An *In Vitro* Study. *J. periodontology* 73 (11), 1292–1298. doi:10.1902/jop.2002.73.11.1292

Li, Q., Chen, Y., Dong, S., Liu, S., Zhang, X., Si, X., et al. (2017). Laser Irradiation Promotes the Proliferation of Mouse Pre-osteoblast Cell Line MC3T3-E1 through Hedgehog Signaling Pathway. *Lasers Med. Sci.* 32 (7), 1489–1496. doi:10.1007/s10103-017-2269-8

Mastrangelo, F., Quaresima, R., Canullo, L., Scarano, A., Muzio, L. L., and Piattelli, A. (2020). Effects of Novel Laser Dental Implant Microtopography on Human Osteoblast Proliferation and Bone Deposition. *Int. J. Oral Maxillofac. Implants* 35 (2), 320–329. doi:10.11607/jomi.7606

Matys, J., Flieger, R., Tenore, G., Grzech-Leśniak, K., Romeo, U., and Dominiak, M. (2018). Er:YAG Laser, Piezosurgery, and Surgical Drill for Bone Decortication during Orthodontic Mini-Implant Insertion: Primary Stability Analysis-An Animal Study. *Lasers Med. Sci.* 33 (3), 489–495. doi:10.1007/s10103-017-2381-9

Mellado-Valero, A., Buitrago-Vera, P., Sola-Ruiz, M., and Ferrer-Garcia, J. (2013). Decontamination of Dental Implant Surface in Peri-Implantitis Treatment: a Literature Review. *Med. Oral* 18 (6), e869–e876. doi:10.4317/medoral.19420

Mordon, S., Brisot, D., and Fournier, N. (2003). Using a ?non Uniform Pulse Sequence? Can Improve Selective Coagulation with a Nd:YAG Laser (1.06 ?m) Thanks to Met-Hemoglobin Absorption: A Clinical Study on Blue Leg Veins. *Lasers Surg. Med.* 32 (2), 160–170. doi:10.1002/lsm.10135

Nejem Wakim, R., Namour, M., Nguyen, H., Peremans, A., Zeinoun, T., Vanheusden, A., et al. (2018). Decontamination of Dental Implant Surfaces by the Er:YAG Laser Beam: A Comparative *In Vitro* Study of Various Protocols. *Dent. J.* 6 (4), 66. doi:10.3390/dj6040066

Niimi, H., Ohsugi, Y., Katagiri, S., Watanabe, K., Hatasa, M., Shimohira, T., et al. (2020). Effects of Low-Level Er:YAG Laser Irradiation on Proliferation and Calcification of Primary Osteoblast-like Cells Isolated from Rat Calvaria. *Front. Cell. Dev. Biol.* 8, 459. doi:10.3389/fcell.2020.00459

Ninomiya, T., Miyamoto, Y., Ito, T., Yamashita, A., Wakita, M., and Nishisaka, T. (2003). High-intensity Pulsed Laser Irradiation Accelerates Bone Formation in Metaphyseal Trabecular Bone in Rat Femur. *J. bone mineral metabolism* 21 (2), 67–73. doi:10.1007/s007740300011

Pantawane, M. V., Chipper, R. T., Robertson, W. B., Khan, R. J., Fick, D. P., and Dahotre, N. B. (2019). Evolution of Surface Morphology of Er: YAG Laser-Machined Human Bone. *Lasers Med. Sci.* 35, 1–9. doi:10.1007/s10103-019-02927-w

Pourzarandian, A., Watanabe, H., Aoki, A., Ichinose, S., Sasaki, K. M., Nitta, H., et al. (2004). Histological and TEM Examination of Early Stages of Bone Healing after Er:YAG Laser Irradiation. *Photomed. Laser Surg.* 22 (4), 342–350. doi:10.1089/pho.2004.22.342

Romanos, G. E., Motwani, S. V., Montanaro, N. J., Javed, F., and Delgado-Ruiz, R. (2019). Photothermal Effects of Defocused Initiated versus Noninitiated Diode Implant Irradiation. *Photobiomodulation, Photomed. laser Surg.* 37 (6), 356–361. doi:10.1089/photob.2018.4545

Safioti, L. M., Kotsakis, G. A., Pozhitkov, A. E., Chung, W. O., and Daubert, D. M. (2017). Increased Levels of Dissolved Titanium Are Associated with Peri-Implantitis - A Cross-Sectional Study. *J. periodontology* 88 (5), 436–442. doi:10.1902/jop.2016.160524

Santos, M. I., and Reis, R. L. (2010). Vascularization in Bone Tissue Engineering: Physiology, Current Strategies, Major Hurdles and Future Challenges. *Macromol. Biosci.* 10 (1), 12–27. doi:10.1002/mabi.200900107

Schwarz, F., Bieling, K., Nuesry, E., Sculean, A., and Becker, J. (2006). Clinical and Histological Healing Pattern of Peri-Implantitis Lesions Following Non-surgical Treatment with an Er:YAG Laser. *Lasers Surg. Med.* 38 (7), 663–671. doi:10.1002/lsm.20347

Sennerby, L., and Meredith, N. (2008). Implant Stability Measurements Using Resonance Frequency Analysis: Biological and Biomechanical Aspects and Clinical Implications. *Periodontol. 2000* 47 (1), 51–66. doi:10.1111/j.1600-0757.2008.00267.x

Trisi, P., Berardini, M., Falco, A., and Vulpiani, M. P. (2015). Effect of Temperature on the Dental Implant Osseointegration Development in Low-Density Bone. *Implant Dent.* 24 (1), 96–100. doi:10.1097/id.0000000000000204

Van Nimwegen, S. A., L'eplattenier, H. F., Rem, A. I., Van Der Lugt, J. J., and Kirpensteijn, J. (2008). Nd:YAG Surgical Laser Effects in Canine Prostate Tissue: Temperature and Damage Distribution. *Phys. Med. Biol.* 54 (1), 29–44. doi:10.1088/0031-9155/54/1/003

Vescovi, P., Meleti, M., Merigo, E., Manfredi, M., Fornaini, C., Guidotti, R., et al. (2013). Case Series of 589 Tooth Extractions in Patients under Bisphosphonates Therapy. Proposal of a Clinical Protocol Supported by Nd:YAG Low-Level Laser Therapy. *Med. Oral* 18 (4), e680–e685. doi:10.4317/medoral.18812

Yin, K., Zhu, R., Wang, S., and Zhao, R. C. (2017). Low-level Laser Effect on Proliferation, Migration, and Antiapoptosis of Mesenchymal Stem Cells. *Stem cells Dev.* 26 (10), 762–775. doi:10.1089/scd.2016.0332

Zavan, B., Ferroni, L., Gardin, C., Sivolella, S., Piattelli, A., and Mijiritsky, E. (2017). Release of VEGF from Dental Implant Improves Osteogenetic Process: Preliminary *In Vitro* Tests. *Materials* 10 (9), 1052. doi:10.3390/ma10091052